

## Supporting Information

### **High-performance piezoelectric nanogenerators based on hierarchical ZnO@CF/PVDF composite film for self-power meteorological sensor**

Yinhui Li<sup>a\*</sup>, Jiaojiao Sun<sup>a</sup>, Pengwei Li<sup>a</sup>, Xuran Li<sup>a</sup>, Jianqiang Tan<sup>a</sup>, Hulin Zhang<sup>a</sup>, Tingyu Li<sup>a</sup>, Jianguo Liang<sup>b</sup>, Yunlei Zhou<sup>c</sup>, ZhenYin Hai<sup>d\*</sup> and Jin Zhang<sup>e\*</sup>

<sup>a</sup> Micro-Nano System Research Center, College of Information and Computer, Taiyuan University of Technology, Taiyuan 030024, Shanxi, Republic of China

<sup>b</sup> College of Mechanical and Vehicle Engineering, Taiyuan University of Technology, Taiyuan 030001, Shanxi, Republic of China.

<sup>c</sup> Hangzhou Institute of Technology, Xidian University, Hangzhou, 311231, Zhejiang, Republic of China

<sup>d</sup> Department of Mechanical and Electrical Engineering, School of Aerospace Engineering, Xiamen University, Xiamen 361005, Republic of China.

<sup>e</sup> Shanxi Bethune Hospital, Shanxi Academy of Medical Sciences, Third Hospital of Shanxi Medical University, Taiyuan, 030032, Shanxi. Republic of China.

Corresponding author email: [liyinhui@tyut.edu.cn](mailto:liyinhui@tyut.edu.cn); [haizhenyin@xmu.edu.cn](mailto:haizhenyin@xmu.edu.cn); Zhangjin\_99@126.com.

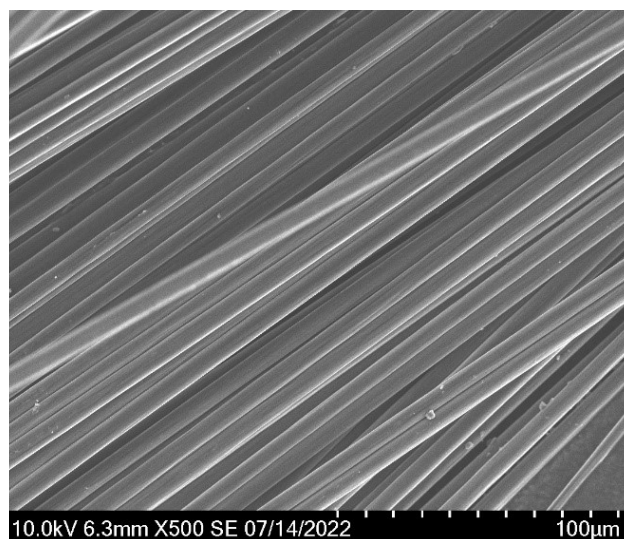


**Fig. S1** SEM images of carbon fiber.

The surface morphology of short chopped carbon fiber (CF) was characterized by SEM. Fig. S1 shows the SEM images of untreated CF. As shown in Fig. S1, the surface of the CF appeared neat and smooth. A few narrow parallel grooves distributed along the fiber's longitudinal way, owing to the manufacture process of CF.<sup>1</sup> The diameter of CF is uniform and average diameter of CF is about 7.0  $\mu\text{m}$ .

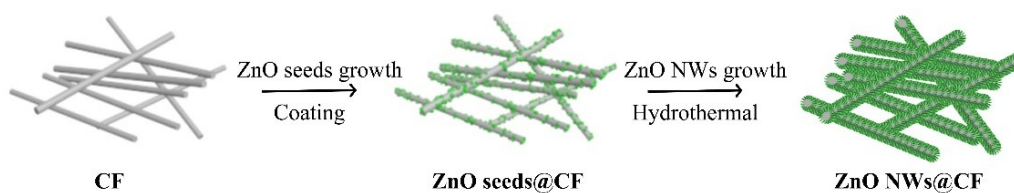


**Fig. S2** Schematic illustration of the fabrication for ZnO@CF hierarchical composite fiber

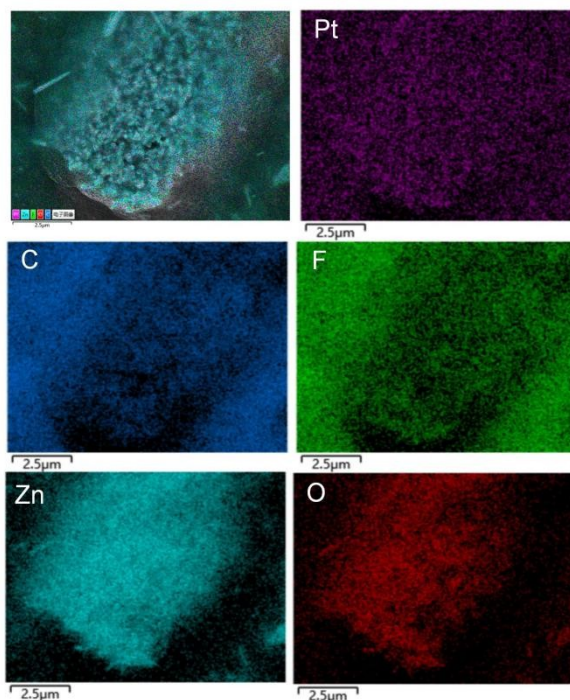


**Fig. S3** SEM image and elemental mapping of C, F, Zn, O and Pt corresponding to the SEM image

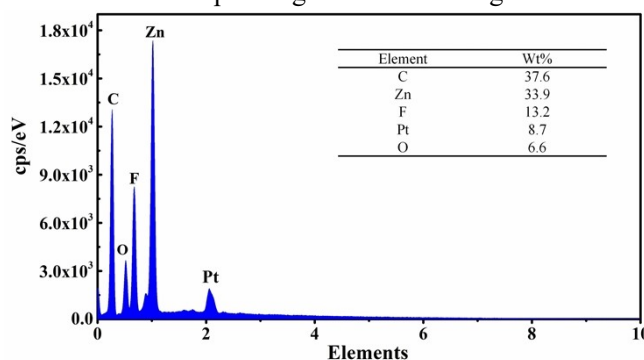


**Fig. S4** EDS analysis of the ZnO@CF/PVDF composite film

The elemental mapping of ZnO@CF/PVDF has been characterized by Energy Dispersive Spectroscopy (EDS). Typical SEM-EDS maps surface of the ZnO@CF/PVDF composite film are shown in Fig. S3. It is found that the presence of C, F, Zn, O elements and the presence of Pt is because of the composite film were sputter-coated by gold particles before observation. Fig. S4 displays the amounts of C, F, Zn, O and Pt (wt%) which are major elemental components in the composite film except Pt. The elemental maps reveal that C and F are evenly distributed on the surface of composite film, and Zn and O are retained rod-like structure indicate that the ZnO@CF with PVDF have been successfully compounded and the hetero-architectural structure of ZnO@CF has been maintained in PVDF matrix.

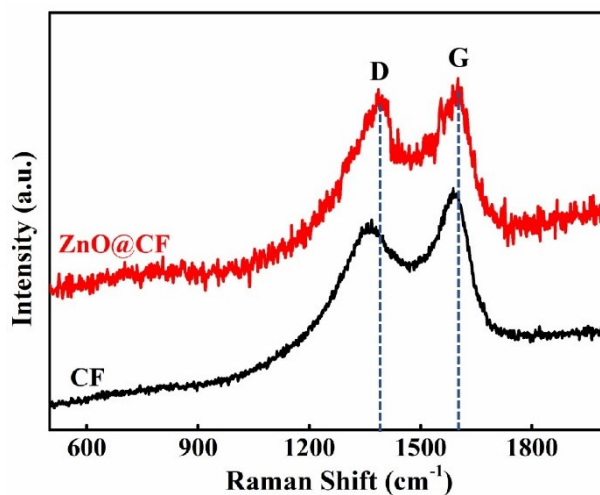


**Fig. S5** Raman spectra of CF and ZnO@CF.

Raman spectra of CF and ZnO@CF are displayed in Fig. S5. CF showed two different bands at  $\sim 1361\text{ cm}^{-1}$ , which attributed to a defected  $\text{sp}^2$  hybridization of carbon “D-band” and  $\sim 1582\text{ cm}^{-1}$ , which attributed in-plane vibrations of the graphite “G-band”, respectively. After ZnO NWs covered on CF, the position of D band and G band shift to  $1383\text{ cm}^{-1}$  and  $1596\text{ cm}^{-1}$ , respectively. The change of band positions indicates the destruction of the graphitic structure.<sup>2</sup>

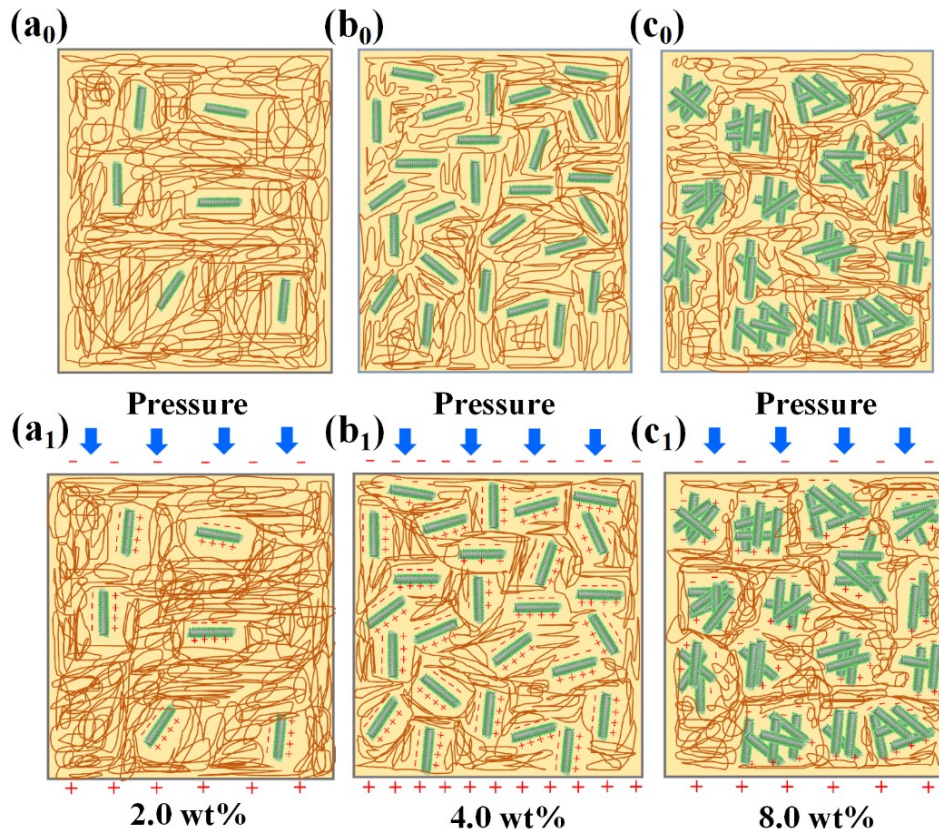


**Fig. S6** The mechanism of piezoelectric charge generating of ZnO@CF/PVDF with the ZnO@CF content of 2.0, 4.0 and 8.0wt%

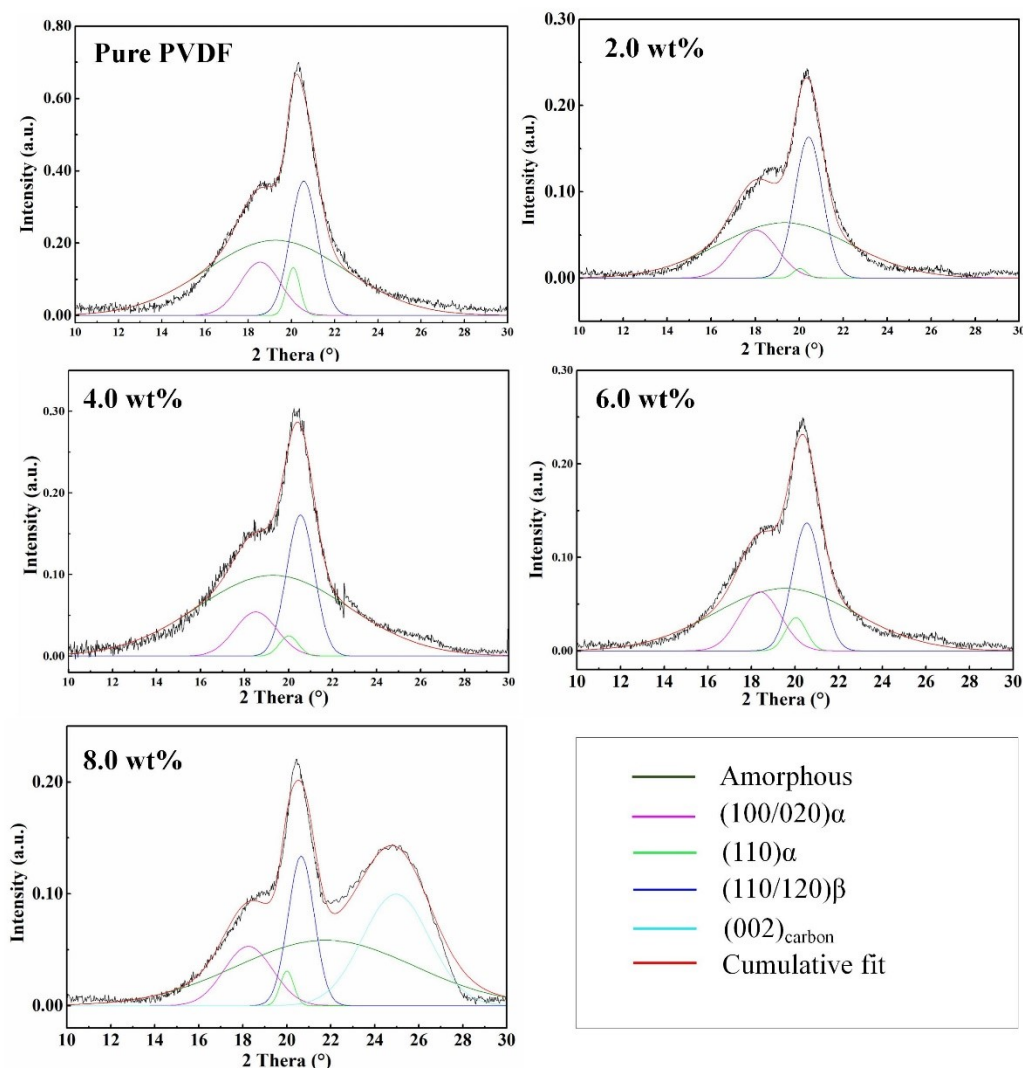


**Fig. S7** XRD peak fitting of ZnO@CF/PVDF composite film with different content of ZnO@CF 0 wt%, 2.0 wt%, 4.0 wt%, 6.0 wt% and 8.0 wt%

In order to characterize the evolution of the  $\beta$  phase fraction influenced by introduction different concentration ZnO@CF, the x-ray profiles were fitted with a sum of Gaussians, corresponding to the crystal and the amorphous phases respectively, and an automatic constant baseline subtraction according to previous work.<sup>3</sup> The crystal and amorphous peaks' fitted results are shown in Fig. S7. In Fig. S7, the broad amorphous peak represents the amorphous phase centered at  $19.3^\circ$  for ZnO@CF/PVDF composite films with 0, 2.0, 4.0, 6.0 wt% and  $21.8^\circ$  for ZnO@CF/PVDF composite films with 8.0 wt%. The peaks  $(100/020)\alpha$  and  $(110)\alpha$  are at  $18.6^\circ$  and  $20.1^\circ$  and represent the convoluted  $(100/020)$  and  $(100)$  diffraction peaks of the  $\alpha$  phase, respectively. The peak  $(100/200)\beta$  is centered at  $20.6^\circ$ , which

represents the convoluted (110/200) diffraction peak of the  $\beta$  phase. From the fit of the X-ray curves, the crystallinity index ( $I_c$ ) was calculated by the formula (1):

$$I_c = \frac{S_{(100/020)\alpha} + S_{(110)\alpha} + S_{(100/200)\beta}}{S_{(100/020)\alpha} + S_{(110)\alpha} + S_{(100/200)\beta} + S_{\text{amorphous}}} \quad (1)$$

The ratio of the  $\beta$  crystal was calculated by the formula (2):

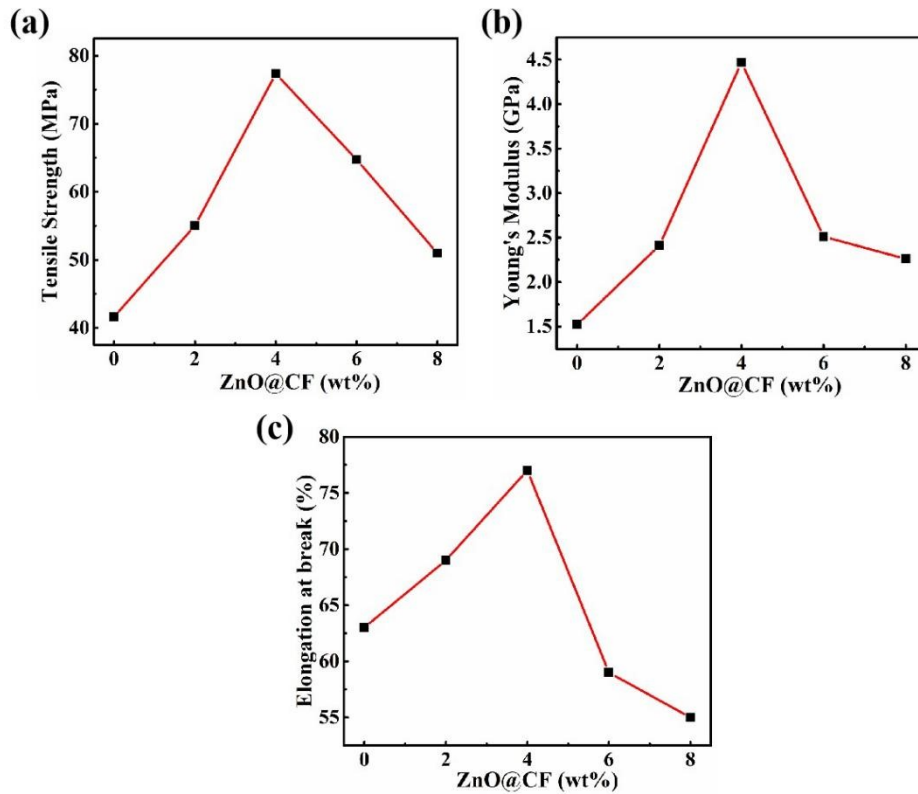
$$\beta = \frac{S_{(100/200)\beta}}{S_{(100/020)\alpha} + S_{(110)\alpha} + S_{(100/200)\beta}} \quad (2)$$

Where  $S_{(100/020)\alpha}$  and  $S_{(110)\alpha}$  is peak area (100/020) $\alpha$  and (110) $\alpha$  are at 18.6° and 20.1° for  $\alpha$  phase;  $S_{(100/200)\beta}$  is peak area (100/200) $\beta$  at 20.6° for  $\beta$  phase;  $S_{\text{amorphous}}$  is the peak area of amorphous.

The calculated results of  $I_c$  and mass ratio of the  $\beta$  crystal are listed in Table R1. From Table R1, the value of  $I_c$  are similar ~40 % for all ZnO@CF/PVDF composite samples which indicated that the introduction of ZnO@CF almost has little influence on the crystallinity index. However, the value of ratio of  $\beta$  crystal first increase and then decrease as the increasing of ZnO@CF content. when the ZnO@CF content increase from 0 to 2.0 to 4.0 wt%, the ratio of the  $\beta$  crystal value increase from 56.5 to 62.3 to 66.5 %. While the ZnO@CF content increase from 6.0 to 8.0 wt%, the ratio of the  $\beta$  crystal value decrease from 64.4 to 53.8 %. Though the values of  $\beta$  phase calculated by XRD pattern is slightly lower than that calculated by FTIR in our manuscript owing to the existence of errors in fitting process, those fitting results has the same vary tendency compare to the calculated result of  $F(\beta)$  in our manuscript, which indicated the content of  $\beta$  phase increased due to an introduction of ZnO@CF in our work is convincing.

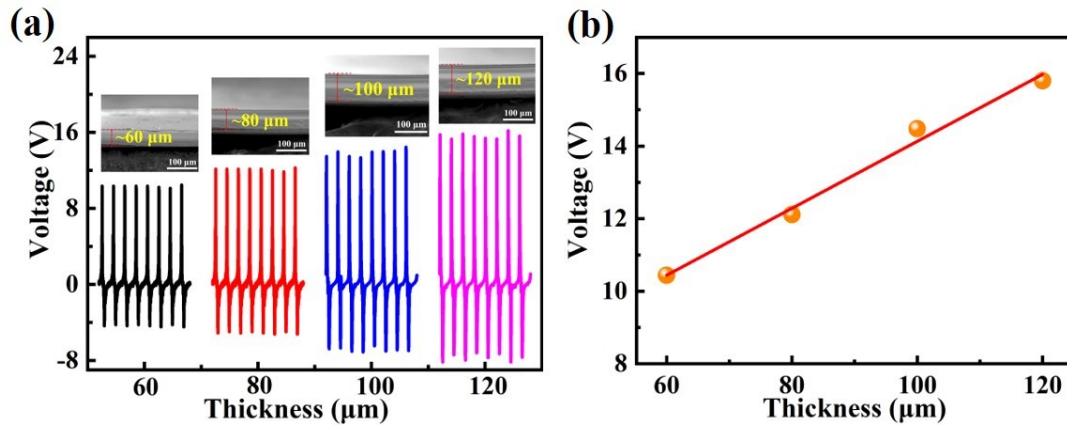
**Table S1**  $I_c$  and ratio of  $\beta$  crystal for ZnO@CF/PVDF composite film with different content of ZnO@CF

Sample code	$I_c^{a*}(\%)$	$\beta^{b*}(\%)$
Pure PVDF	38.3	56.5
ZnO@CF/PVDF-2.0 wt%	40.2	62.3
ZnO@CF/PVDF-4.0 wt%	38.7	66.5
ZnO@CF/PVDF-6.0 wt%	39.0	64.4
ZnO@CF/PVDF-8.0 wt%	38.8	53.8



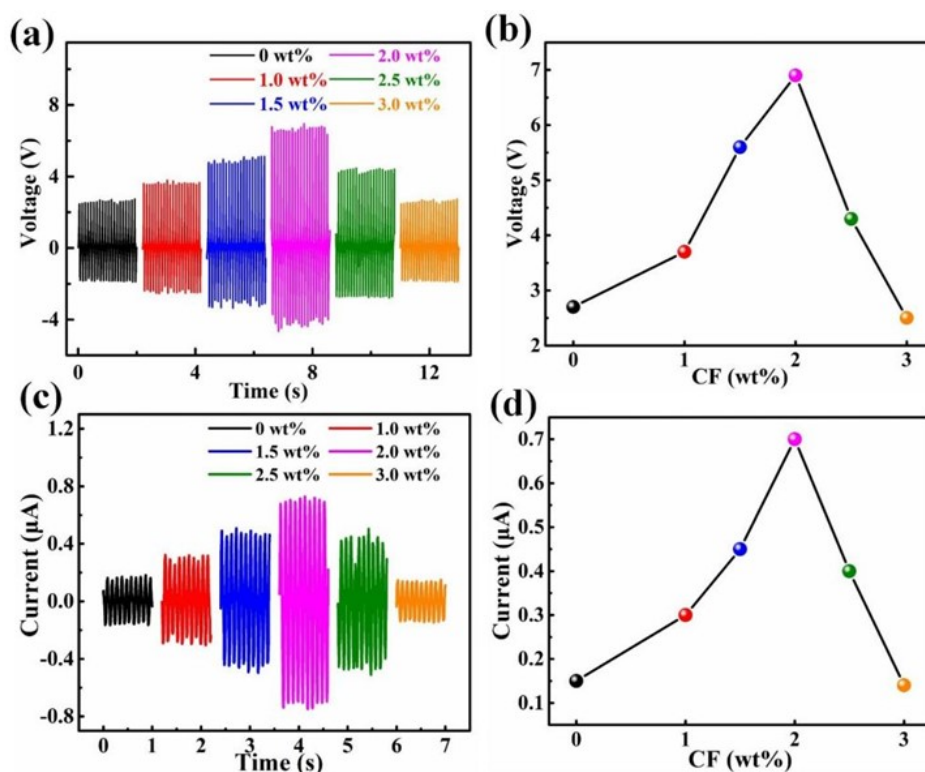
**Fig. S8** Mechanical properties of ZnO@CF/PVDF composite film versus the content of ZnO@CF (a) tensile strength; (b) Young's Modulus; (c) elongation at break

Fig. S8 shows the mechanical properties including tensile strength, Young's Modulus and elongation at break of ZnO@CF/PVDF composite film with different ZnO@CF content. The tensile strength increases from 41.62 to 55.03 to 77.37 MPa, when the content of ZnO@CF increases from 0 to 2.0 to 4.0 wt%. While that value decreases from 64.73 to 55.03 MPa, when the content of ZnO@CF continue increases from 6.0 to 8.0 wt%. The Young's Modulus increases from 1.52 to 2.41 to 4.47GPa, when the content of ZnO@CF increases from 0 to 2.0 to 4.0 wt%. While that value decreases from 2.51 to 2.26 GPa, when the content of ZnO@CF continue increases from 6.0 to 8.0 wt%. Besides, the elongation at break increases from 63 to 69 to 77 %, when the content of ZnO@CF increases from 0 to 2.0 to 4.0 wt%. While that value decreases from 59 to 55 %, when the content of ZnO@CF continue increases from 6.0 to 8.0 wt%. The tensile strength, Young's Modulus and elongation at break of ZnO@CF/PVDF composite film obey the similar rule, it can be concluded for first increase and then decrease with the content of ZnO@CF increasing.



**Fig. S9** The output voltage of pure ZnO@CF/PVDF film with different thickness 60, 80, 100, 120  $\mu\text{m}$  and the insets show the SEM image for different thickness film.

To investigate the influence of thickness on output performance, the output voltage of ZnO@CF/PVDF with different thickness 60, 80, 100, 120  $\mu\text{m}$  were obtained. The ZnO@CF content was chosen as 4.0 wt% in the composite film. The thickness of ZnO@CF/PVDF composite film were measured by SEM, the results are shown in Fig. S6a. From Fig. S9a, the output voltage of ZnO@CF/PVDF piezoelectric nanogenerator increase from 10.4 to 11.6 to 14.7 to 16.1 V as the thickness of ZnO@CF/PVDF film increasing from 60 to 80 to 100 to 120  $\mu\text{m}$ . Plot of the maximum value of voltage and thickness of piezoelectric film fitting curve is displayed by orange line-symbol in Fig. S9b. The maximum output voltage value linear increases with the thickness increasing under the same mechanical applied stress. In this work, the film thickness of 100  $\mu\text{m}$  has been chosen to obtain flexible and relative excellent output performance.



**Fig. S10** The output performance of the CF/PVDF composite PNGs (CF concentration: 0 wt %; 1.0 wt %; 1.5 wt %; 2.0 wt %; 2.5 wt %; 3.0 wt %) (a) and (b) output voltage; (c) and (d) output current.

Time-dependent output voltage of CF/PVDF composite film piezoelectric nanogenerators were measured under cyclic pressing and releasing beating acceleration  $120 \text{ m/s}^2$  at a frequency of 10 Hz. The open-circuit voltage of PVDF/CF composite film was shown in Fig. S10. From Fig. S10, when the content CF increase from 0 to 1.0 to 1.5 to 2.0 wt%, the output voltage increases from 2.71 V to 3.73 V to 5.65 V to 6.92 V and the output current increases from 0.15 to 0.30 to 0.45 to 0.71  $\mu\text{A}$ , respectively. The chopped CF as conductive phase in piezoelectric to improve the migration rate of the polarization charges. When chopped short CF content is below 2.0 wt%, the output voltage and current enhanced. However, When the chopped short CF increase from 2.5 to 3.0 wt%, the output voltage decreases from 4.32 to 2.51 V and the output current decreases from 0.40 to 0.14  $\mu\text{A}$ . The decrement of output performance is ascribed to the conductivity and leakage current increasing with the excessive chopped short CF doping.

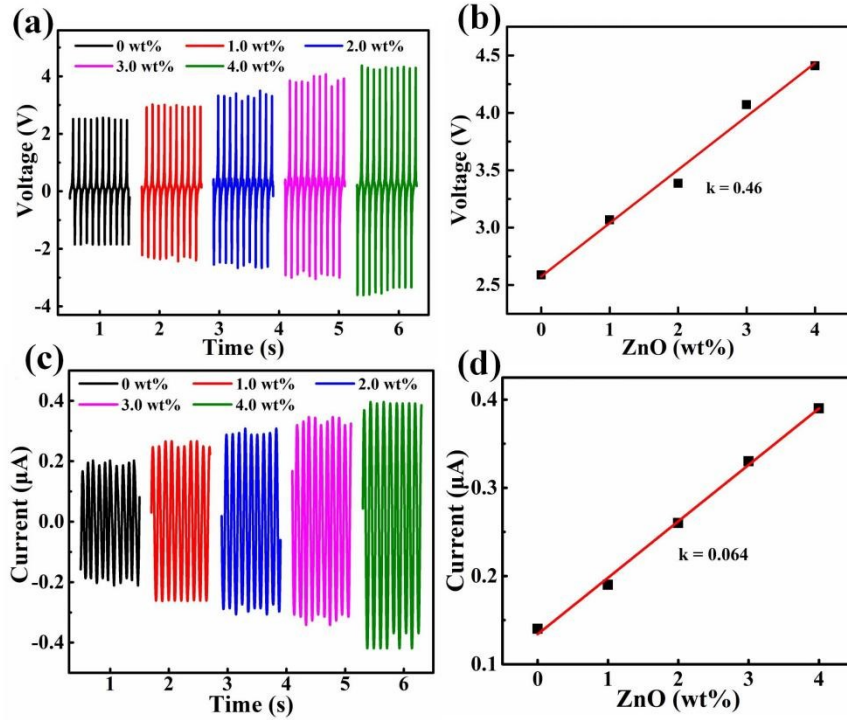


**Fig. S11** Piezoelectric output characteristics of ZnO NW/PVDF composite film PNG (ZnO concentration: 0 wt %; 1.0 wt %; 2.0 wt %; 3.0 wt %; 4.0 wt %): (a) and (b) output voltage; (c) and (d) output current

To evaluate the influence of ZnO NW additive content on output performance on ZnO NW/PVDF composite nanogenerator. Time-dependent output voltage of ZnO NW/PVDF composite film piezoelectric nanogenerators were measured under cyclic pressing and releasing beating acceleration  $120 \text{ m/s}^2$  at a frequency of 10 Hz. The open-circuit voltage and short-circuit current of ZnO NW/PVDF composite films were shown in Fig. S11. From Fig. S11a and b, the output voltage of ZnO NW/PVDF composite piezoelectric nanogenerator increased from 2.71 to 3.09 to 3.41 to 4.05 to 4.41 V when the ZnO NW content increase from 0 to 1.0 to 2.0 to 3.0 to 4.0 wt%. From Fig. S11c and d, the output current of ZnO NW/PVDF composite piezoelectric nanogenerator increased from 0.15 to 0.19 to 0.28 to 0.32 to 0.39  $\mu\text{A}$  as the ZnO NW content increase from 0 to 1.0 to 2.0 to 3.0 to 4.0 wt%. The output voltage and current are linearly correlated with the ZnO NW content, and the linear slope of the voltage and current versus ZnO NW content is 0.46 V/wt% and 0.064  $\mu\text{A/wt\%}$ , respectively. Owing to the piezoelectric coefficient of ZnO NW ( $\sim 110 \text{ pC/m}^2$ ) is much higher than that of PVDF ( $\sim 12 \text{ pC/m}^2$ ). To maintain flexibility of ZnO NW/PVDF composite film, the ZnO NW additive content value is 4.0 wt%. Those results demonstrate CF and ZnO

NW both have an effect on the output performance of CF/PVDF or ZnO NW/PVDF composite film PNG, however, the output voltage and current of CF/PVDF or ZnO NW/PVDF composite film PNG is lower than ZnO NW@CF/PVDF composite film PNG (voltage~14.91 V, current~1.25  $\mu$ A).

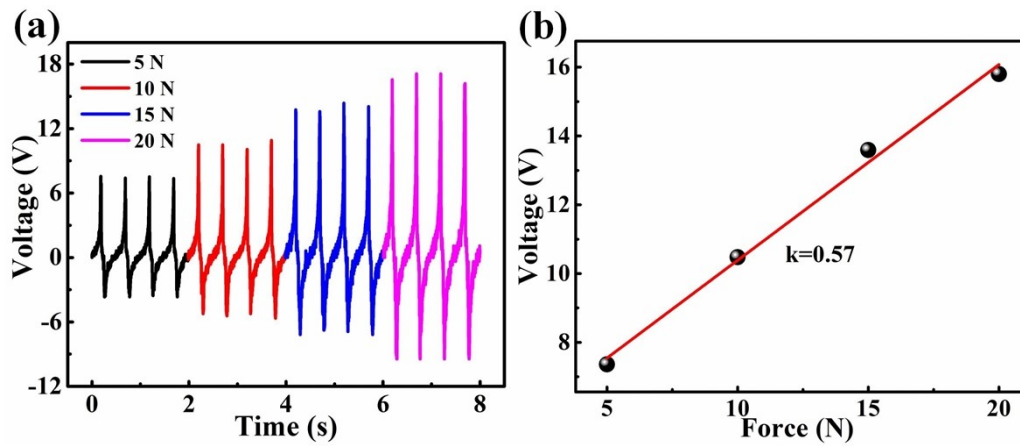


**Fig. S12** (a) Output voltage of ZnO@CF/PVDF composite film PNG under different pressing force; (b) plot of voltage and force fitting curve.

The electrical performance of PNG under a function of loading forces at a fixed frequencies ( $\sim 2$  Hz) has been measured by our typical testing system in our previous work.<sup>4</sup> The output voltage of ZnO@CF/PVDF composite film PNG with ZnO@CF mass fraction 4.0 wt% increased from 7.4 to 10.4 to 13.2 to 16.1 V with the external beaten force increased from 5 to 10 to 15 to 20 N (Fig. S12a). The piezoelectric sensitivity of ZnO@CF/PVDF composite film PNG device can be obtained by the of the linear fitting plot (voltage vs force, Fig. S12b), and the slope of fitting plot is 0.57 V/N.

**Table S2** Summary of dielectric constant at different testing frequency and parameter for plot of fitting curves for ZnO@CF/PVDF composite film.

ZnO@CF (wt%)	Frequency (Hz)					Fitting curve equation $Y = aX + b$		
	$10^2$	$10^3$	$10^4$	$10^5$	$10^6$	a	b	R <sup>2</sup>
0	9.6	8.2	7.1	6.4	6.0	1.90	10.2	0.9919
2.0	13.9	13.0	12.2	11.3	9.9	1.94	8.98	0.9902
4.0	18.8	17.9	17.2	16.3	15.1	1.97	8.05	0.9883
6.0	22.1	21.1	20.3	19.4	18.0	1.95	7.24	0.9880
8.0	24.5	23.6	22.8	21.9	20.5	1.86	6.47	0.9909

\*Fitting curve equation  $Y = aX + b$ , where a is the slop of fitting curve in Fig. 6b, and b is the intercept, R<sup>2</sup> is the standard Error of fitting curve.

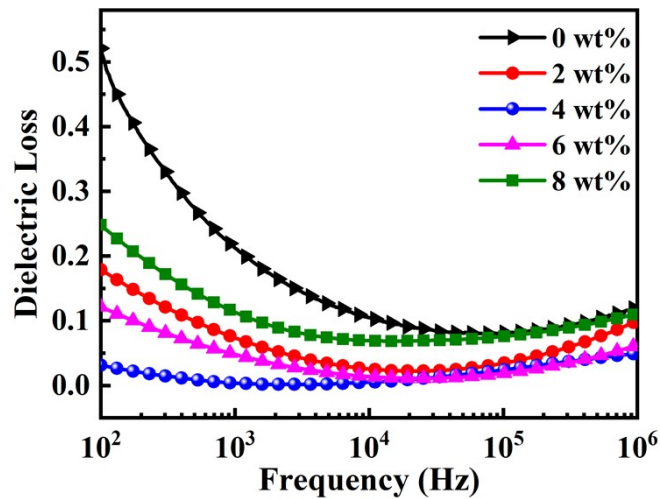


**Fig. S13** The dielectric loss of ZnO@CF/PVDF composite thin films with different ZnO@CF content at different frequencies

The dielectric loss of the ZnO@CF/PVDF composite thin films with different ZnO@CF content (2.0, 4.0, 6.0 and 8.0 wt%) were measured at a frequency of ( $10^2 \sim 10^6$ ) Hz, and compared to that of the pure PVDF are as shown in Fig. S13. Fig. S13 gives the dielectric loss of ZnO@CF/PVDF composite thin films with different ZnO@CF content at different frequencies, which indicates that compared with pristine PVDF film, adding ZnO@CF can effectively reduce the dielectric loss, particularly at low frequencies corresponding to the Maxwell–Wagner relaxation loss or free charge conductivity loss.<sup>5</sup>

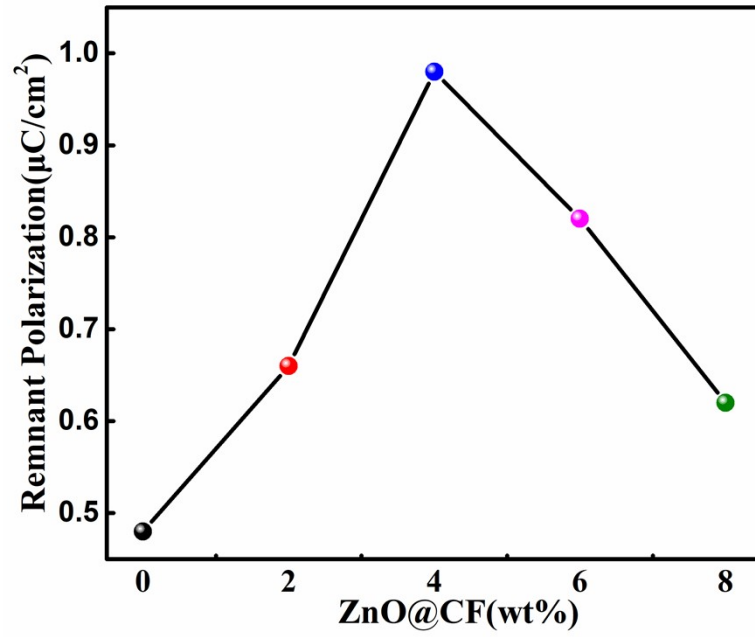


Fig. S14 Variation of the remnant polarization of the ZnO@CF/PVDF composite film with the content of the ZnO@CF

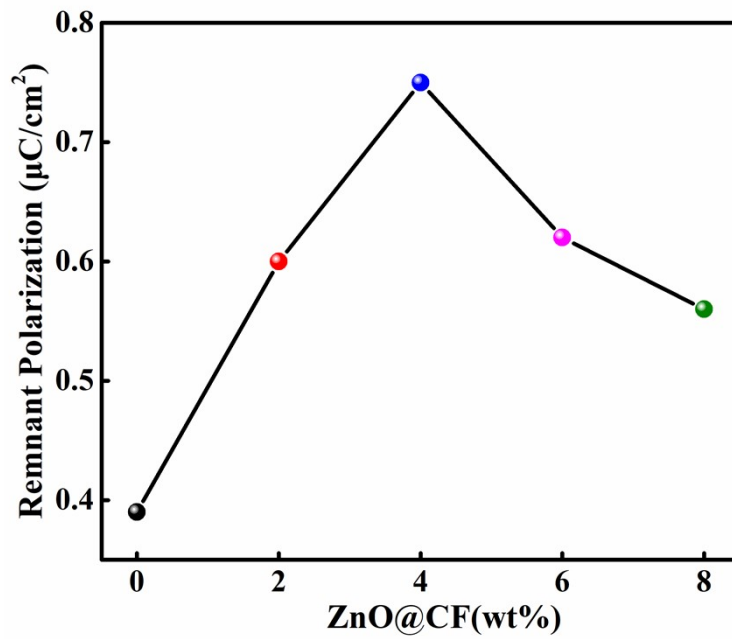
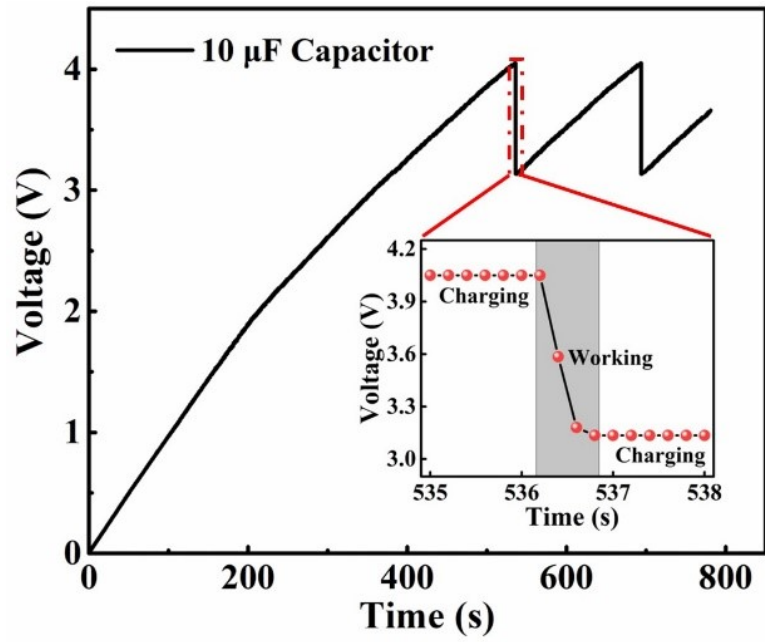
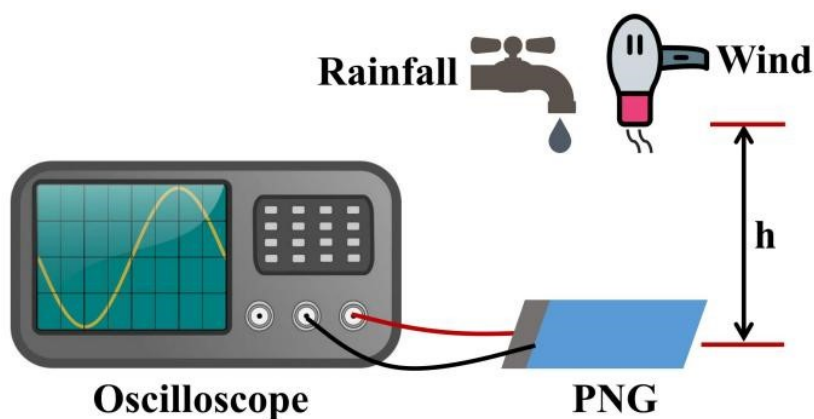


Fig. S15 Variation of the maximum polarization of the ZnO@CF/PVDF composite film with the content of the ZnO@CF



**Fig. S16** Charging of energy storage capacitor by periodic beating, and enlarge view of discharging in insert image.



**Fig. S17** Diagram of simulated meteorological monitoring sensor testing circuit

The output signal of simulated meteorological monitoring sensor was measured by a test system built in our lab. The ZnO@CF/PVDF PNG was beaten repeatedly by water droplets and wind during test. The schematic diagram of test system was as follow in Fig. S17. The output signal of ZnO@CF/PVDF simulated meteorological monitoring sensor was recorded via the oscilloscope through channel 1. Rainfall was simulated by changing the falling rate of the water droplets, and wind was simulated by changing the blowing speed of hair dryer, which indicate this ZnO@CF/PVDF composite film PNG could real-time monitor the rainfall and wind weather as a meteorological sensor.

## Reference

- 1 F. Zhao, Y. Huang, L. Liu, Y. Bai and L. Xu, *Carbon*, 2011, **49**, 2624-2632.
- 2 Q. Ji, X. Zhao, H. Liu, L. Guo and J. Qu, *ACS Appl. Mater. Interfaces*, 2014, **6**, 9496-9502.
- 3 L. Yu, P. Cebe, *Polymer*, 2009, **50(9)**, 2133–2141.
- 4 X. Li, Y. Li, Y. Li, J. Tan, J. Zhang, H. Zhang, J. Liang, T. Li, Y. Liu, H. Jiang, P. Li. *ACS Appl. Mater. Interfaces*, 2022, **14**, 46789-46800.
- 5 L. Yang, Q. Zhao, K. Chen, Y. Ma, Y. Wu, H. Ji and J. Qiu, *ACS Appl. Mater. Interfaces*, 2020, **12**, 11045-11054.